



Published in final edited form as:

Bioorg Med Chem Lett. 2011 May 1; 21(9): 2697–2701. doi:10.1016/j.bmcl.2010.12.015.

Discovery and optimization of a novel, selective and brain penetrant M₁ positive allosteric modulator (PAM): the development of ML169, an MLPCN Probe

Paul R. Reid^{e,†}, Thomas M. Bridges^{a,d,†}, Douglas J. Sheffler^{a,c}, Hyekyung P. Cho^{a,d}, L. Michelle Lewis^e, Emily Days^e, J. Scott Daniels^{a,c,d}, Carrie K. Jones^{a,c,d,f}, Colleen M. Niswender^{a,c,d}, C. David Weaver^{a,d,e}, P. Jeffrey Conn^{a,c,d}, Craig W. Lindsley^{a,b,c,d,e}, and Michael R. Wood^{a,c,d}

^aDepartment of Pharmacology, Vanderbilt University Medical Center, Nashville, TN 37232, USA

^bDepartment of Chemistry, Vanderbilt University, Nashville, TN 37232, USA

^cVanderbilt Program in Drug Discovery, Nashville, TN 37232, USA

^dVanderbilt Specialized Chemistry Center(MLPCN), Nashville, TN 37232, USA

^eVanderbilt Institute of Chemical Biology/Chemical Synthesis Core, Nashville, TN 37232, USA

^fU.S. Department of Veterans Affairs, Tennessee Valley Healthcare System, Nashville, TN 37212, USA

Abstract

This Letter describes a chemical lead optimization campaign directed at VU0108370, a weak M₁ PAM hit with a novel chemical scaffold from a functional HTS screen within the MLPCN. An iterative parallel synthesis approach rapidly established SAR for this series and afforded VU0405652 (ML169), a potent, selective and brain penetrant M₁ PAM with an in vitro profile comparable to the prototypical M₁ PAM, BQCA, but with an improved brain to plasma ratio.

The muscarinic acetylcholine receptors (mAChRs) are members of the family A G-protein-coupled receptors (GPCRs) and include five subtypes denoted M₁-M₅. All five of the mAChRs are known to play critical roles in multiple basic physiological processes and represent attractive therapeutic targets for a number of peripheral and CNS pathologies.¹⁻³ Within the mAChRs, a major challenge has been a lack of subtype selective ligands to study the specific contribution of discrete mAChRs in various disease states.³⁻⁴ To address this limitation, we have focused on targeting allosteric sites on mAChRs as a means to develop subtype selective small molecules, both allosteric agonists and positive allosteric modulators (PAMs).⁵⁻⁹ Moreover, the emerging phenomenon of ligand-biased signaling requires the development of diverse chemical scaffolds of M₁ ligands to successfully dissect of the roles of M₁ activation through multiple, discrete ligand-biased signaling pathways.¹⁰⁻¹¹

As members of the Molecular Libraries Production Center Network (MLPCN),¹² we performed a real-time cell-based calcium-mobilization assay employing a rat M₁/CHO cell

Correspondence to: Michael R. Wood.

[†]these authors contributed equally to this work

Publisher's Disclaimer: This is a PDF file of an unedited manuscript that has been accepted for publication. As a service to our customers we are providing this early version of the manuscript. The manuscript will undergo copyediting, typesetting, and review of the resulting proof before it is published in its final citable form. Please note that during the production process errors may be discovered which could affect the content, and all legal disclaimers that apply to the journal pertain.

line (Z' averaged 0.7) and screened a 63,656 member MLPCN compound library following a triple-add protocol to simultaneously identify M_1 antagonists, agonists (both orthosteric and allosteric) and positive allosteric modulators (PAMs). This screen proved to be a major success providing viable leads that were optimized into potent and highly selective M_1 ligands (Fig. 1): an M_1 antagonist (**1**, VU0255035, ML012),¹³ an M_1 allosteric agonist (**2**, VU0357017, ML071),¹⁴ and both an M_1 PAM (**3**, VU0366369, ML137)¹⁵ and the first M_5 PAM (**4**, VU0238429, ML129)¹⁶ derived from a pan- M_1, M_3, M_5 -PAM (**5**, VU0119498).¹⁷⁻¹⁸ However, the brain penetration ($\text{brain}_{AUC}/\text{plasma}_{AUC} = 0.1$) and efficacy (60% ACh Max) of **3** were poor, as was the brain penetration of the prototypical M_1 PAM, BQCA (**6**, $\text{brain}_{AUC}/\text{plasma}_{AUC} = 0.1$)¹⁹⁻²¹; therefore, M_1 PAM ligands with improved physicochemical properties for *in vivo* studies and novel scaffolds to address ligand-biased signaling are required. In this Letter, we describe the development of VU0405652 (ML169), a highly selective M_1 PAM MLPCN probe, with a novel chemical scaffold and improved brain penetration.

Perusal of the HTS data, which also yielded the non-selective hit **5**, identified a second weak M_1 PAM hit **7**, VU0108370, with an EC_{50} of $\sim 13 \mu\text{M}$. Confirmation of **7** from fresh powder and counter-screening against M_2 - M_5 increased our enthusiasm for this highly M_1 mAChR selective hit (Fig. 2); however, the CRC did not plateau, suggesting the M_1 EC_{50} was actually $>13 \mu\text{M}$. Despite the weak potency, the confirmation of a novel M_1 PAM scaffold with high M_1 selectivity initiated a lead optimization campaign to improve M_1 potency while maintaining the high M_2 - M_5 selectivity.

Our initial optimization strategy is outlined in Figure 3, and as SAR with allosteric ligands is often shallow, we employed an iterative parallel synthesis approach, along with targeted syntheses for structures encompassing more speculative modifications. Attempted modifications of the Eastern oxazole-amide, although not extensive, met with no success, returning only compounds with undetectable activity. In a straightforward attempt to reduce molecular weight the benzyl group attached to the indole nitrogen was omitted, but met with a similar lack of success ($EC_{50} > 10 \mu\text{M}$) as did the sulfide and sulfoxide congeners.

Thus, we planned to hold the northern portion of **7** constant, and survey diversity on the southern benzyl moiety employing a library synthesis approach. As shown in Scheme 1, the key library scaffold **12** was readily prepared in 3 steps from methyl thioglycolate **8**. A PyClu-mediated microwave-assisted coupling between **9** and **10** provided **11** in 71% yield, which was then oxidized to the corresponding sulfone **12** with Oxone in 88% yield. An 18-membered library of analogs **13** was then prepared by treatment with NaH and 18 diverse benzyl halides.

As shown in Table 1, SAR, as with many allosteric ligands, was shallow affording only five active compounds from the eighteen synthesized. Upon resynthesis, HTS hit **7** (a 2-Cl congener) showed an EC_{50} of $9.7 \mu\text{M}$ with 83% ACh Max; however, the CRC once again did not plateau. The other four actives, all with substituents in the 3-position, did afford sigmoidal CRCs with up to 96% ACh Max and EC_{50} s in the 3.8 to $6.5 \mu\text{M}$ range. The most potent analog was **13g**, a 3-Br derivative ($EC_{50} = 3.8 \mu\text{M}$, 91% ACh Max) which provided a significant increase in potency, but at the cost of physicochemical properties ($c\text{LogP} > 4$ and poor solubility). Replacement of the benzyl moiety with a pyridyl analog also led to an inactive compound (data not shown). However, this first generation library indicated that substitution at the 3-position of the benzyl moiety was preferred. This result then prompted us to employ **13g** as a starting material for a small Suzuki coupling library (Scheme 2) to replace the lipophilic bromide with various aryl and heteroaryl moieties to introduce basicity and/or polarity.

As shown in Table 2, SAR was again shallow, but we identified pyrazole as a preferred heterocyclic replacement for the bromide. *N*-Me pyrazole **14a** possessed an M₁ EC₅₀ of 3.2 μM (102% ACh Max), while the unsubstituted pyrazole congener **14b** was essentially equipotent (M₁ EC₅₀ = 2.2 μM, 90% ACh Max). Moreover, both pyrazole congeners lowered cLogP a full order of magnitude relative (cLogP = 3.1) to **13g**. Additional steric bulk on the pyrazole, as in the *sec*-butyl derivative **14c**, led to an inactive analog. Phenyl derivative **14d** and basic amino pyridine analogs **14e-14h**, were inactive (M₁ EC₅₀s >10 μM).

To further the development of this novel series of M₁ PAMs we focused on three of the more potent analogs (**13a**, **13g** and **14b**) and applied a fine-tuning process of introducing fluorine atoms at various locations to provide analogs **15** (Table 3), an approach we found successful for multiple allosteric ligands. Across the series, substitution at the 4-position was uniformly not tolerated (**15a-c**), consistent with the SAR appearing in Table 1. Bis-fluorination of the indole ring eroded activity in the context of the bromine analog **15d** but conversely augmented the activity of the pyrazole congener **15e**. This type of subtle/confounding SAR was similarly observed with respect to fluorination at the R² position in analogs **15f-h**. While the presence of a fluorine at R² was neutral or slightly beneficial in the context of the chlorine analog (**15f**), its presence resulted in clearly decreased activity for both the bromine and pyrazole analogs, **15g** and **15h**. Lastly, the introduction of a single fluorine at the R⁶ position could either be moderately detrimental in the context of pyrazole **15i** or decidedly beneficial with respect to bromine analog **15j**, where an almost 3-fold improvement in potency was observed. In this manner, both VU0405652 (**15j**) and the related difluorindole analog VU0405645 (**15e**) were chosen for further evaluation.

Both **15e** and **15j** were selective (Fig. 4A) for M₁ (>30 μM vs. M₂-M₅) and both compounds demonstrated impressive left-ward shifts of the ACh CRC (98-fold and 49-fold, respectively) in fold-shift assays at 30 μM (Fig. 4B), values comparable to BQCA. However, a combination of calculated properties (TPSA, Hacc, etc...), ancillary pharmacology and *in vivo* PK suggested **15j** was the more optimal MLPCN probe molecule compared to **15e**.

In terms of ancillary pharmacology, the Lead Profile screen at Ricerca, evaluating 68 GPCRs, ion channels and transporters in radioligand binding assays, resulted in only two significant activities (DAT, 83% at 10 μM and sodium channel site 2, 83% at 10 μM); importantly, **15j** was selective versus the biogenic amines (D₂, H-HT₂B, etc...) and displayed no orthosteric binding at M₁-M₅. Based on the exciting *in vitro* profile, we then evaluated **15j** for brain penetration in rat. A 10 mg/kg IP dose of **15j** afforded a brain_{AUC}/plasma_{AUC} of 0.32 at 1 hour, providing an improvement over both **3** (ML137) and BQCA with brain_{AUC}/plasma_{AUC} of ~0.1. Based on this profile, **15j** (VU0405652) was declared an MLPCN probe, ML169.

As we have previously demonstrated with both an M₁ PAM (BQCA)²⁰ and M₁ allosteric agonists (**2**, ML071 and TBPB),²³ ML169 also shifted APP processing towards a non-amyloidogenic pathway.²⁴ As shown in Figure 5, 10 μM carbachol (CCh) affords a significant increase in soluble APP (APP_s), while 100 nM CCh provides a modest increase. VU0405652 (ML169) at a dose of 2 μM has no effect, but in combination with low dose CCh (100 nM), ML169 potentiates the CCh-mediated non-amyloidogenic APP_s release to the same degree as 10 μM CCh. These data once again suggest that selective activation of M₁ may have a disease modifying role in Alzheimer's disease.^{14,20}

In summary, we have developed a potent, selective and brain penetrant M₁ PAM, ML169, based on a novel indole scaffold from an MLPCN functional HTS. Further *in vivo*

evaluation of this probe is underway and results from preclinical models of Alzheimer's disease and schizophrenia will be reported in due course. ML169 is an MLPCN probe and freely available upon request.

Acknowledgments

The authors thank the MLPCN (1U54 MH084659), NIMH (1RO1 MH082867), NIH and the Alzheimer's Association (IIRG-07-57131) for support of our Program in the development of subtype selective allosteric ligands of mAChRs.

References and Notes

1. Bonner TI, Buckley NJ, Young AC, Brann MR. *Science*. 1987; 237:527–532. [PubMed: 3037705]
2. Bonner TI, Young AC, Brann MR, Buckley NJ. *Neuron*. 1988; 1:403–410. [PubMed: 3272174]
3. Wess J. *Annu Rev Pharmacol Toxicol*. 2004; 44:423–450. [PubMed: 14744253]
4. Langmead CJ, Watson J, Reavill C. *Pharmacol Ther*. 2008; 117:232–243. [PubMed: 18082893]
5. Conn PJ, Jones C, Lindsley CW. *Trends in Pharm Sci*. 2009; 30:25–31. [PubMed: 19058862]
6. Conn PJ, Lindsley CW, Jones C. *Trends in Pharm Sci*. 2009; 30:148–156. [PubMed: 19201489]
7. Conn PJ, Christopoulos A, Lindsley CW. *Nat Rev Durg Disc*. 2009; 8:41–54.
8. Bridges TM, LeBois EP, Hopkins CR, Wood MR, Jones JK, Conn PJ, Lindsley CW. *Drug News & Perspect*. 2010; 23:229–240.
9. Lewis JA, Lebois EP, Lindsley CW. *Curr Opin Chem Biol*. 2008; 12:269–279. [PubMed: 18342020]
10. Digby GJ, Conn PJ, Lindsley CW. *Curr Opin Drug Disc & Dev*. 2010; 13:577–586.
11. Marlo JE, Niswender CM, Luo Q, Brady AE, Shirey JK, Rodriguez AL, Bridges TM, Williams R, Days E, Nalywajko NT, Austin C, Williams M, Xiang Y, Orton D, Brown HA, Kim K, Lindsley CW, Weaver CD, Conn PJ. *Mol Pharm*. 2009; 75(3):577–588.
12. For information on the MLPCN and information on how to request probe compounds, such as ML169, see: <http://mli.nih.gov/mli/mlpcn/>
13. Sheffler DJ, Williams R, Bridges TM, Lewis LM, Xiang Z, Zheng F, Kane AS, Byum NE, Jadhav S, Mock MM, Zheng F, Lewis LM, Jones CK, Niswender CM, Weaver CD, Conn PJ, Lindsley CW, Conn PJ. *Mol Pharmacol*. 2009; 76:356–368. [PubMed: 19407080]
14. Lebois EP, Bridges TM, Dawson ES, Kennedy Jp, Xiang Z, Jadhav SB, Yin H, Meiler J, Jones CK, Conn PJ, Weaver CD, Lindsley CW. *ACS Chemical Neurosci*. 2010; 1:104–121.
15. Bridges TM, Kennedy JP, Cho HP, Conn PJ, Lindsley CW. *Bioorg Med Chem Lett*. 2010; 20:1972–1975. [PubMed: 20156687]
16. Bridges TM, Marlo JE, Niswender CM, Jones JK, Jadhav SB, Gentry PR, Weaver CD, Conn PJ, Lindsley CW. *J Med Chem*. 2009; 52:3445–3448. [PubMed: 19438238]
17. Bridges TM, Kennedy JP, Cho HP, Conn PJ, Lindsley CW. *Bioorg Med Chem Lett*. 2010; 20:558–562. [PubMed: 20004578]
18. Bridges TM, Kennedy JP, Hopkins CR, Conn PJ, Lindsley CW. *Bioorg Med Chem Lett*. 2010; 20:5617–5622. [PubMed: 20801651]
19. Ma L, Seager M, Wittman M, Bickel N, Burno M, Jones K, Graufelds VK, Xu G, Pearson M, McCampbell A, Gaspar R, Shughrue P, Danzinger A, Regan C, Garson S, Doran S, Kreatsoulas C, Veng L, Lindsley CW, Shipe W, Kuduk S, Jacobson M, Sur C, Kinney G, Seabrook GR, Ray WJ. *Proc Natl Acad Sci USA*. 2009; 106:15950–15955. [PubMed: 19717450]
20. Shirey JK, Brady AE, Jones PJ, Davis AA, Bridges TM, Jadhav SB, Menon U, Christain EP, Doherty JJ, Quirk MC, Snyder DH, Levey AI, Watson ML, Nicolle MM, Lindsley CW, Conn PJ. *J Neurosci*. 2009; 29:14271–14286. [PubMed: 19906975]
21. Yang FV, Shipe WD, Bunda JL, Nolt MB, Wisnoski DD, Zhao Z, Barrow JC, Ray WJ, Ma L, Wittman M, Seager M, Koeplinger K, Hartman GD, Lindsley CW. *Bioorg Med Chem Lett*. 2010; 20:531–536. [PubMed: 20004574]

22. **ML169, 2-((1-(5-bromo-2-fluorobenzyl)-1H-indol-3-yl)sulfonyl)-N-(5-methylisoxazol-3-yl)acetamide.** To a solution of indole (3.00 g, 25.6 mmol) and methyl thioglycolate **8** (2.40 mL, 25.6 mmol) in methanol:water (80 mL: 20 mL) was added iodine (6.50 g, 25.6 mmol) and potassium iodide (4.25 g, 25.6 mmol). The reaction mixture was stirred at ambient temperature for 60 hours. Methanol was removed *in vacuo* and the aqueous layer diluted with a saturated solution of sodium bicarbonate and extracted with ethyl acetate. The organic layer was dried over magnesium sulfate, evaporated *in vacuo* and the resulting residue was purified on a silica gel column (0-100% ethyl acetate:hexanes over 33 min) to afford the ester as an oil (LCMS >98%). The ester was dissolved in a mixture of tetrahydrofuran (20 mL) and 2.0M aqueous LiOH (15 mL), then stirred vigorously at ambient temperature for 30 minutes. Tetrahydrofuran was removed *in vacuo*, the aqueous layer neutralized with 1.2 N HCl and extracted with CH₂Cl₂. The organic layer was dried over magnesium sulfate and removed *in vacuo* to produce an oily residue. Upon diluting the residue in dichloromethane a reddish-brown solid formed which was filtered and dried to yield compound **9** (2.00 grams, 9.65 mmol, 38% yield over 2 steps, LCMS >98%). Compound **10** (650 mg, 3.14 mmol), 3-amino-5-methyl-isoxazole (616 mg, 6.28 mmol), PyCIU (2.00 g, 6.28 mmol), and DIEA (1.36 mL, 7.85 mmol) were added to dichloroethane (25 mL) and microwave irradiated at 110 °C for 20 minutes. After cooling, the solvent was removed *in vacuo* and the remaining residue purified on a silica gel column (0-70% ethyl acetate:hexanes over 33 min) to yield compound **11** (642 mg, 2.23 mmol, 71% yield, LCMS >98%). Compound **11** (502 mg, 1.77 mmol) was dissolved in 25 mL (9:1, methanol:water) and Oxone (10.0 g, 17.7 mmol) was added. Stirring at ambient temperature continued overnight. Water (20 mL) was added and the mixture extracted with ethyl acetate (3×20 mL). The organics were combined, dried over magnesium sulfate, and concentrated *in vacuo* to give an oily residue which was purified on silica gel (0-50% ethyl acetate:hexanes over 19 min) to yield compound **12** (500 mg, 1.57 mmol, 88% yield, LCMS >98%). In a 5 mL microwave vial, compound **12** (55.0 mg, 0.174 mmol) was dissolved in DMF (3 mL) and cooled to 0 °C. Sodium hydride (60% by weight, 14.0 mg, 0.348 mmol) was then added in one portion and the reaction mixture vigorously stirred at 0 °C for 15 minutes. 4-bromo-2-bromomethyl-1-fluorobenzene (51.0 mg, 0.191 mmol) was added in one portion and the reaction mixture was stirred while being allowed to warm to ambient temperature over 3 hours. The reaction mixture was quenched with water (2 mL) and the solution was extracted with ethyl acetate (3×4 mL). The combined organics were dried over magnesium sulfate, concentrated *in vacuo* to give an oily residue which was purified on silica gel (0-70% ethyl acetate:hexanes over 19 min) to yield **ML169** (45 mg, 0.088 mmol, 51% yield). LCMS >98% 214 nm, R_T = 1.34 min, m/z = 506 ([⁷⁹Br]m+1), 508 ([⁸¹Br]m+1). ¹H NMR (400 MHz, DMSO-*d*₆) 11.27 (s, 1H), 8.23 (s, 1H), 7.82 (d, *J* = 8.0 Hz, 1H), 7.63 (d, *J* = 8.0 Hz, 1H), 7.56-7.58 (m, 1H), 7.47 (dd, *J* = 2.4 Hz, 6.4 Hz, 1H), 7.35-7.23 (m, 3H), 6.54 (s, 1H), 5.62 (s, 2H), 4.43 (s, 2H), 2.37 (s, 3H), HRMS found: 506.0184; calculated for C₂₁H₁₇BrFN₃O₄S: 506.0185.
23. Jones CK, Brady AE, Davis AA, Xiang Z, Bubser M, Tantawy MN, Kane A, Bridges TM, Kennedy JP, Bradley SR, Peterson T, Baldwin RM, Kessler R, Deutch A, Lah JL, Levey AI, Lindsley CW, Conn PJ. *J Neurosci.* 2008; 28(41):10422–10433. [PubMed: 18842902]
24. *APP processing.* In order to test the effect of M₁ PAM on M₁-stimulated APPs_a release, a human M1 overexpressing stable cell line was generated in TReX293 cells (Invitrogen). Cells were plated at 0.3×10⁶ cells in 6-well plate 2 days prior to experiments. Cells were pretreated with 2μM VU0405652 or dimethylsulfoxide (DMSO) for 15 min. Immediately, 100nM or 10μM carbachol was added, and the medium was then conditioned for 1 h at 37°C. Western blot analysis of the endogenous APPs_a in conditioned media was performed as described.²³

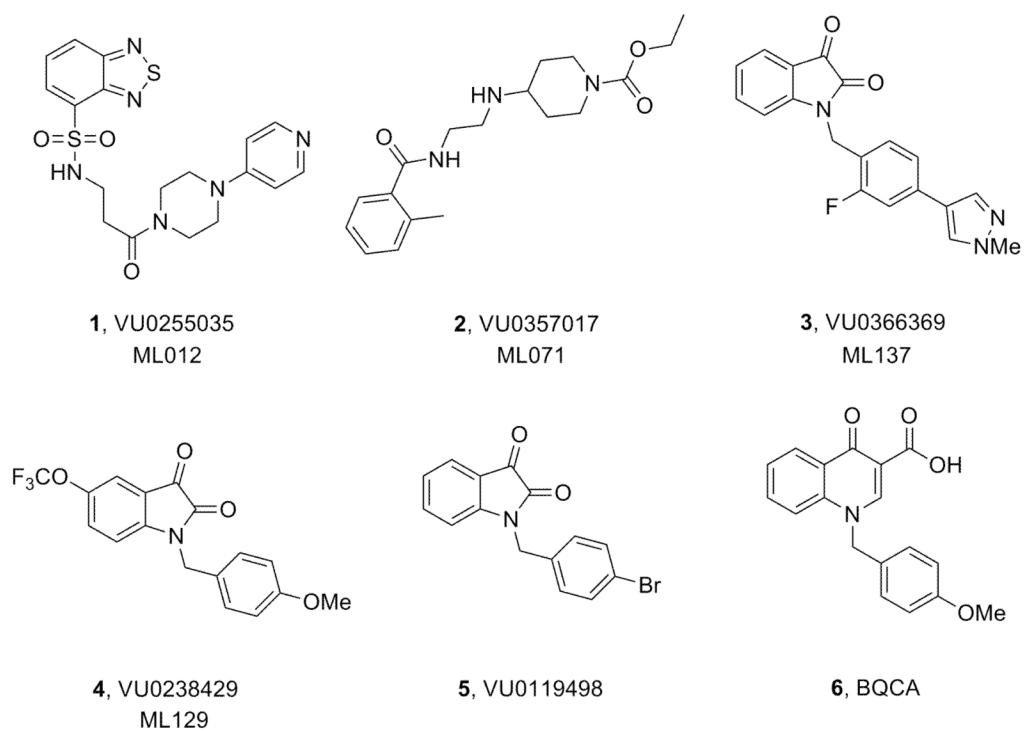


Figure 1. Structures of selective M₁ and M₅ MLPCN probes developed from hits from a triple-add functional M₁ HTS MLPCN screen (**1-5**) and BQCA (**6**).

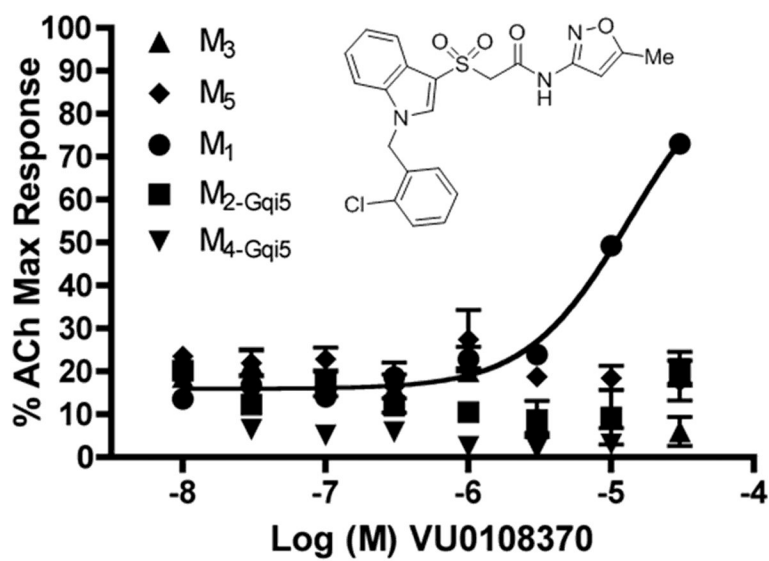


Figure 2. Concentration response curves (CRCs) for M₁-M₅ for HTS hit VU0108370. M₁ EC₅₀ ~13 μ M (does not plateau) and M₂-M₅ EC₅₀ >30 μ M.

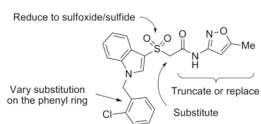


Figure 3.
Initial optimization strategy for VU0108370, **7**.

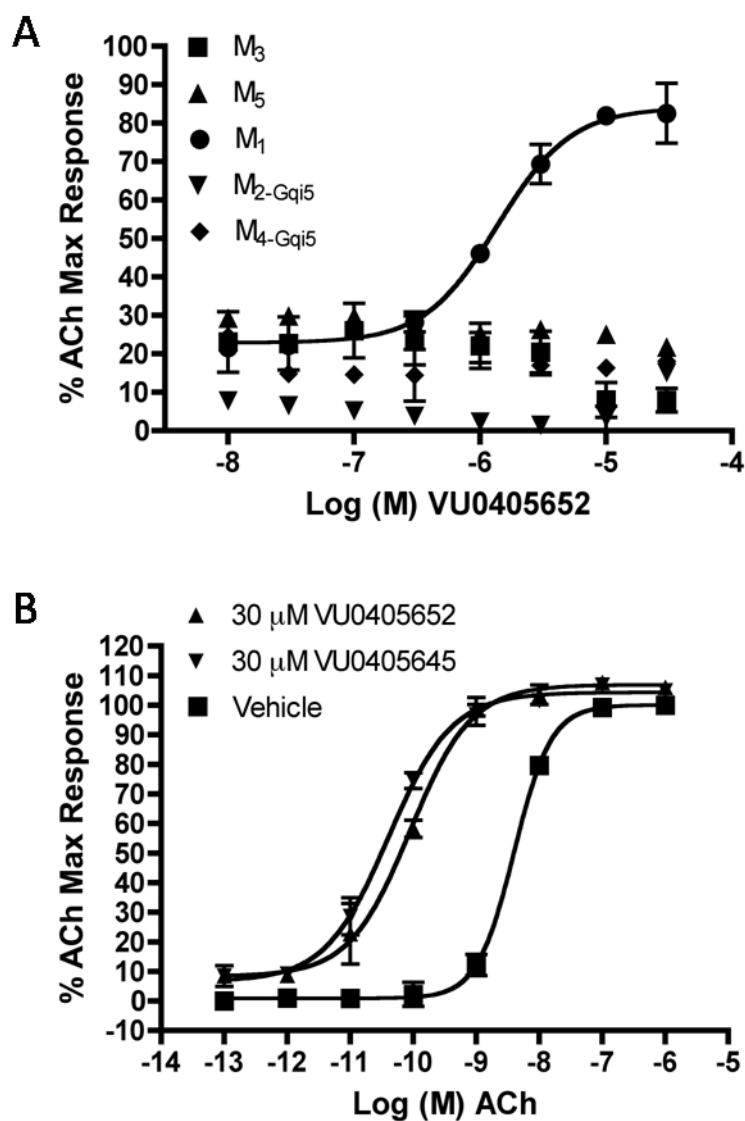


Figure 4.
 A) CRC for **15j**, VU0405652 at M₁-M₅ (**15e**, VU0405645 looked similar); B) ACh fold-shift experiment at 30 μM for VU0405652 (49-fold) and VU0405645 (98-fold).

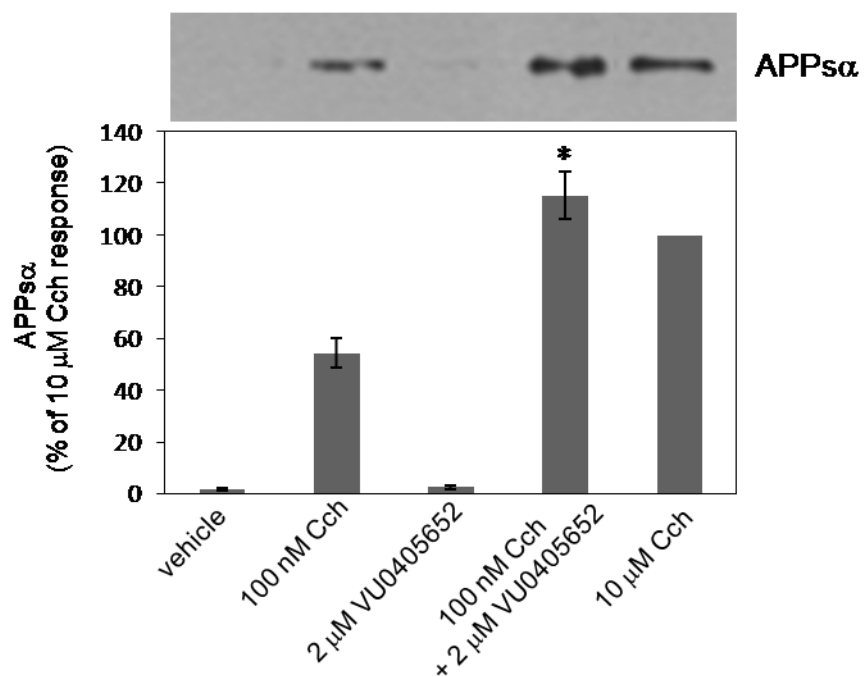
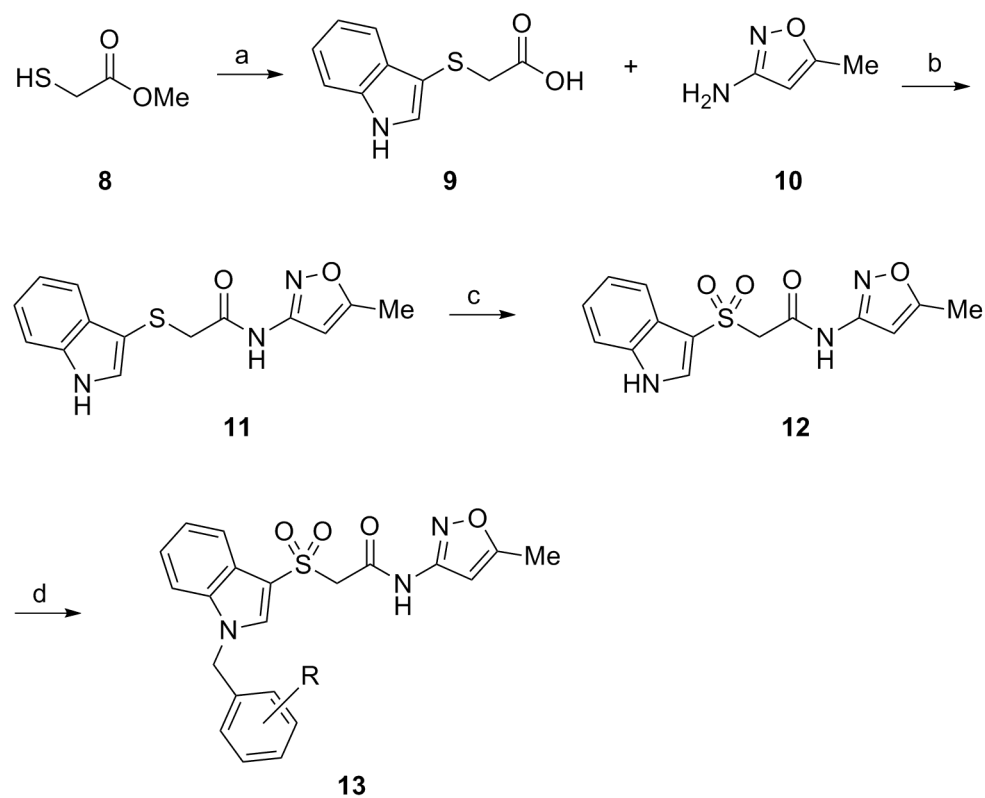
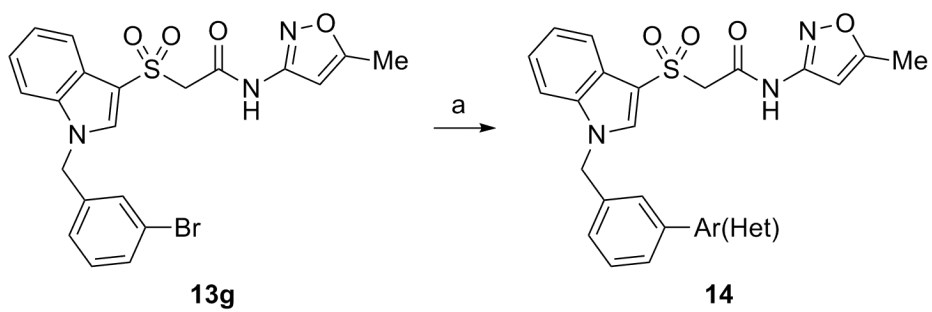


Figure 5. M₁ PAM VU04505652 (ML169) potentiates the CCh-mediated non-amyloidogenic APPs α release in TReX293-hM₁ cells.

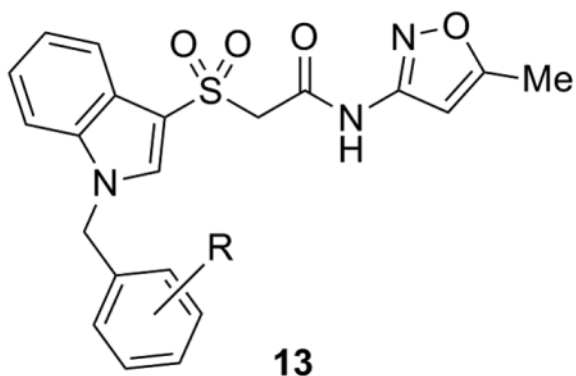
**Scheme 1.**

Reagents and conditions: (a) i. indole, I₂, KI, MeOH, H₂O; ii. 2M LiOH, THF (38%); (b) PyClu, DCE, 110 °C, 20 min, mw (71%); (c) Oxone, MeOH, H₂O (88%); NaH, DMF, BnX (50-90%).

**Scheme 2.**

Reagents and conditions: (a) Ar-B(OH)₂ or Het-B(OH)₂, 10 mol % Pd(*t*-Bu)₂, 1.0 M aq Cs₂CO₃, THF, mw, 120 °C (65-90%).

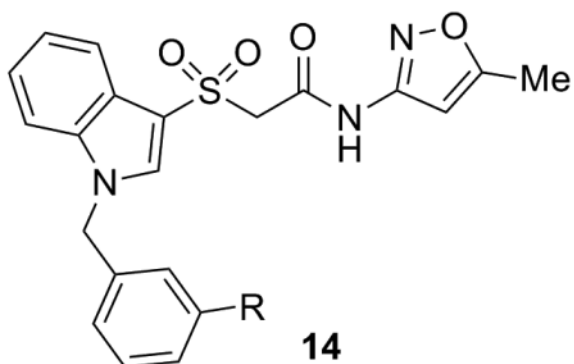
Table 1

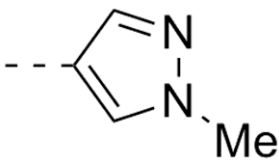
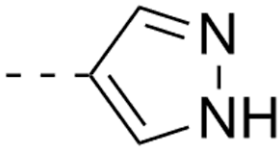
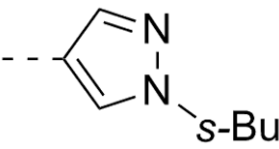
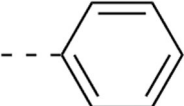
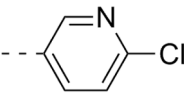
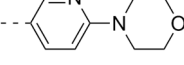
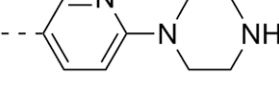
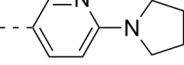
Structures and activities of analogs **13**.

Cmpd	R	M ₁ EC ₅₀ (μM) ^a	%ACh Max ^a
7	2-Cl	9.71	83
13a	3-Cl	5.82	96
13b	4-Cl	>10	-
13c	2-OMe	>10	-
13d	3-OMe	6.54	79
13e	4-OMe	>10	-
13f	3-F	5.22	96
13g	3-Br	3.79	91
13h	3-CF ₃	>10	-
13i	3-CN	>10	-
13j	3,5-diBr	>10	-
13k	3,4-diCl	>10	-
13l	4-CF ₃	>10	-
13m	4-OCF ₃	>10	-
13n	2-F	>10	-
13o	2,4-diF	>10	-
13p	2-Br-4-F	>10	-

^a Average of at least three independent determinations.

Table 2

Structures and activities of analogs **14**.

Cmpd	Ar/Het	M ₁ EC ₅₀ (μM) ^a	%ACh Max ^a
14a		3.21	102
14b		2.19	90
14c		>10	-
14d		>10	-
14e		>10	-
14f		>10	-
14g		>10	-
14h		>10	-

^a Average of at least three independent determinations

Table 3

Structures and activities of analogs **15**.

Cmpd	G	R ¹	R ²	R ³	R ⁴	R ⁵	R ⁶	M ₁ EC ₅₀ (μM) ^a	%ACh Max ^a
15a	A	H	H	F	H	H	H	>10	-
15b	Br	H	H	F	H	H	H	>10	-
15c	Cl	H	H	F	H	H	H	>10	-
15d	Br	F	H	H	H	H	H	5.37	103
15e	A	F	H	H	H	H	H	1.85	102
15f	Cl	H	F	H	H	H	H	5.10	56
15g	Br	H	F	H	H	H	H	>10	-
15h	A	H	F	H	H	H	H	4.40	103
15i	A	H	H	H	H	F	F	3.07	96
15j	Br	H	H	H	H	F	F	1.38	84

^a Average of at least three independent determinations.